

Efficient and flexible spatiotemporal clutter filtering of high frame rate images using subspace tracking

B.S. Generowicz*, G. Leus*, S. Soloukey Tbalvandany^{†‡}, W.S. van Hoogstraten[†], C. Strydis[†], J.G. Bosch[§], A.F.W. van der Steen[§], C. I. de Zeeuw^{†¶}, S.K.E. Koekkoek[†], and P. Kruizinga^{†§}

*Faculty of Electrical Engineering, Mathematics and Computer Science, Delft University of Technology, Delft, the Netherlands

[†]Department of Neuroscience, Erasmus Medical Center, Rotterdam, the Netherlands

[‡]Department of Neurosurgery, Erasmus Medical Center, Rotterdam, the Netherlands

[§]Department of Biomedical Engineering, Erasmus Medical Center, Rotterdam, the Netherlands

[¶]Netherlands Institute of Neuroscience, Royal Dutch Academy for Arts and Sciences, Amsterdam, the Netherlands

Abstract—Current methods to measure blood flow using ultrafast Doppler imaging often make use of a Singular Value Decomposition (SVD). The SVD has been shown to be an effective way to remove clutter signals associated with slow moving tissue. Conventionally, the SVD is calculated from an ensemble of frames, after which the first dominant eigenvectors are removed. The Power Doppler Image (PDI) is then computed by averaging over the remaining components. The SVD method is computationally intensive and lacks flexibility due to the fixed ensemble length. We propose a method, based on the Projection Approximation Subspace Tracking (PAST) algorithm, which is computationally efficient and allows us to sequentially estimate and remove the principal components, while also offering flexibility for calculating the PDI, e.g. by using any convolutional filter. During a functional ultrasound (fUS) measurement, the intensity variations over time for every pixel were correlated to a known stimulus pattern. The results show that for a pixel chosen around the location of the stimulation electrode, the PAST algorithm achieves a higher Pearson correlation coefficient than the state-of-the-art SVD method, highlighting its potential to be used for fUS measurements.

Index Terms—clutter filter, functional ultrasound, subspace tracking, Doppler imaging.

I. INTRODUCTION

Ultrafast Doppler imaging has gained popularity due to its high temporal resolution which is beneficial to distinguishing blood motion from slow moving tissue. High spatio-temporal resolution is achieved by insonifying the whole field-of-view in a single shot using planewave transmissions at several thousand Hertz [1]. Multiple angled planewaves can be coherently compounded to compensate for the loss of performance when a single planewave is used [2].

There are various methods that can be used to extract the blood-flow signal contained in the ultrasound data. Based on the assumption that tissue and blood signal have different temporal characteristics, it is possible to use FIR or IIR filters, however, due to the varying tissue and blood characteristics over space and time, these types of filters can be difficult to optimize [3]. More recently, the Singular Value Decomposition (SVD) has been shown to be effective at suppressing clutter signals while maintaining high spatio-temporal resolution [4].

An ensemble of ultrasound images are reshaped to form a 2D-space-time matrix of dimensions $(n_z \times n_x, n_e)$ where n_z , n_x and n_e represent the number of samples in the space-depth, space-width (along the transducer array) and time direction respectively. This matrix is decomposed using an SVD to form an ordered and weighted sum of separable matrices, as

$$\mathbf{S} = \sum_{k=1}^{n_e} \lambda_k \mathbf{u}_k \mathbf{v}_k^* \quad (1)$$

Here, \mathbf{u}_k and \mathbf{v}_k are the k^{th} column of the unitary matrices \mathbf{U} and \mathbf{V} with respective dimensions $(n_z \times n_x, n_z \times n_x)$, (n_e, n_e) , and λ_k is the k^{th} ordered singular value of a diagonal matrix $\mathbf{\Delta}$ with dimensions $(n_z \times n_x, n_e)$. Here, \mathbf{u}_k can be represented as a 2D spatial image of dimensions (n_z, n_x) with intensity $|\mathbf{u}_k|$. Baranger *et al.* have shown [5], that due to the different spatial characteristics of tissue and blood signals, the intensity vectors $|\mathbf{u}_k|$ related to tissue signals are correlated to each other. The intensity vectors related to the blood signals are also correlated to each other, however not to the tissue subspace. Therefore, to demonstrate the use of the SVD to segregate tissue and blood signals, the correlation matrix of $|\mathbf{U}|$ was created using a functional ultrasound (fUS) dataset and is shown in Fig. 1. When the images are reconstructed for each of the correlation regions shown, it is clear that the first components represent the slow moving tissue subspace while the other components contain the blood subspace.

A filtered image containing blood flow signal \mathbf{S}^f , can be reconstructed by setting the leading tissue-related diagonal components of the eigenvalue matrix $\mathbf{\Delta}$ to zero to create a filtered version $\mathbf{\Delta}^f$, resulting in

$$\mathbf{S}^f = \mathbf{U} \mathbf{\Delta}^f \mathbf{V}^* \quad (2)$$

To create the final Power Doppler Image (PDI), the filtered image is averaged over the temporal dimension of the 2D-space-time matrix and reshaped to an image of dimensions (n_z, n_x) . Due to the high complexity of the SVD method, this is only repeated once per data ensemble with no overlap (referred to as

batch-SVD). This technique has two major drawbacks: it is 1) computationally intensive, and 2) not flexible, as it requires a fixed ensemble length n_e . To address this problem, we present a computationally efficient method allowing us to sequentially estimate and remove the principal components related to tissue signal, while also offering flexibility for calculating the PDI, as this method is not restricted by a fixed ensemble length.

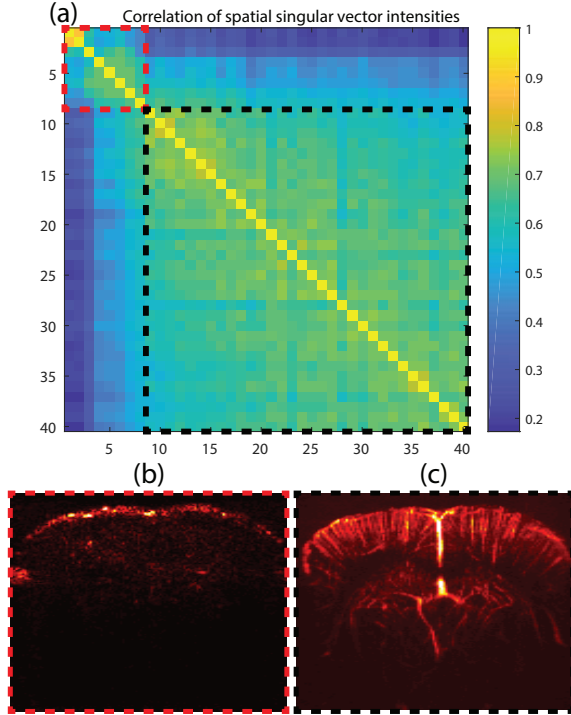


Figure 1: Tissue and blood subspaces contained in ultrafast Doppler imaging. (a) The correlation matrix of the spatial singular vector intensities shows two distinct regions, where the reconstructed PDI of the first segment contains mainly tissue signal and the other segment contains mainly blood signal. (b)-(c) show the eigenvectors 1-9 that span the tissue subspace where components 9-40 contain blood signal.

II. METHODS

A. Functional Ultrasound

The PDIs of a mouse brain were obtained using a 28 MHz linear array transducer coupled to an ultrasound system (Vantage 64-LE). A total of $n = 2$ adult anesthetized C57BL/6 mice (Charles River, NL) were subjected to an electrical stimulation paradigm. After induction (4% isoflurane in O_2), the mice underwent a surgical craniotomy with a pedestal placement, before being head-fixed in the set-up for imaging. During imaging the anesthesia was lowered (1% isoflurane in O_2). Throughout the experiment, body temperature was maintained at 37.6°C.

B. Projection Approximation Subspace Tracking (PAST)

The PAST and PASTd¹ have been developed [6] to track subspaces while having reduced computational complexity and storage requirements as they only work with a small part of the

eigenstructure. As seen in Section I, the first eigencomponents span the tissue subspace, which, therefore, can be effectively removed. As the PASTd algorithm explicitly calculates the eigencomponents, it provides the option of estimating the number of eigencomponents to remove. This flexibility is convenient when the threshold between tissue and blood signal varies over time, as is often the case in Doppler imaging. We therefore chose to focus on the implementation of PASTd in this paper, shown in Algorithm 1. The deflation technique refers to the sequential estimation of the eigencomponents, where $d_i(t)$ is an estimate of the i^{th} eigenvalue and $w_i(t)$ is an estimate of the corresponding eigenvector.

Algorithm 1 PASTd algorithm

```

1: for  $t = 1, 2, \dots$  do
2:    $\mathbf{x}_1(t) = \mathbf{x}(t)$ 
3:   for  $i = 1, 2, \dots, r$  do
4:      $y_i(t) = \mathbf{w}_i^H(t-1)\mathbf{x}_i(t)$ 
5:      $d_i(t) = \beta d_i(t-1) + |y_i(t)|^2$ 
6:      $\mathbf{e}_i(t) = \mathbf{x}_i(t) - \mathbf{w}_i(t-1)y_i(t)$ 
7:      $\mathbf{w}_i(t) = \mathbf{w}_i(t-1) + \mathbf{e}_i(t)[y_i^*/d_i(t)]$ 
8:    $\mathbf{x}_{i+1} = \mathbf{x}_i(t) - \mathbf{w}_i(t)y_i(t)$ 

```

At every iteration, the algorithm has a data vector $\mathbf{x}(t)$ as input, corresponding to a new ultrasound image. The projections of the data vector onto the r most dominant eigencomponents are sequentially removed, leaving a new data vector containing only the components of the blood motion signal. Furthermore, these r most dominant eigenvectors are updated using the new data vector. The PASTd algorithm has a computational complexity of $O(n \times r)$ per image while the SVD method maintains a complexity of $O(n \times n_e^2)$ where n is the length of the data vector and where n_e is the ensemble length.

III. FLEXIBILITY USING PASTD

A. Weighted update

The PASTd algorithm was previously implemented using an exponentially weighted window [6] on the data $\mathbf{x}(t)$. This technique takes into account all previous data and down-weights information from the distant past to allow tracking in non-stationary environments using a forgetting factor $0 < \beta < 1$. Due to the flexibility of the algorithm, it is also possible to implement other windows, such as a fixed length sliding window, where a specified number of previous frames l are weighted equally. This method more closely relates to the batch-SVD method mentioned in Section I. Interestingly, the PASTd-exponential window (PASTd-ew) algorithm is able to remove the tissue subspace with much fewer removed components than the batch-SVD method, as can be seen in the PDIs in Fig. 2. As the complexity of the PASTd algorithm scales with the removed components r , it is beneficial for r to remain small. The PASTd-sliding window (PASTd-sw) method follows a more similar trend to the SVD method, requiring more removed components to display the blood subspace.

¹A modified version of PAST based on the deflation technique

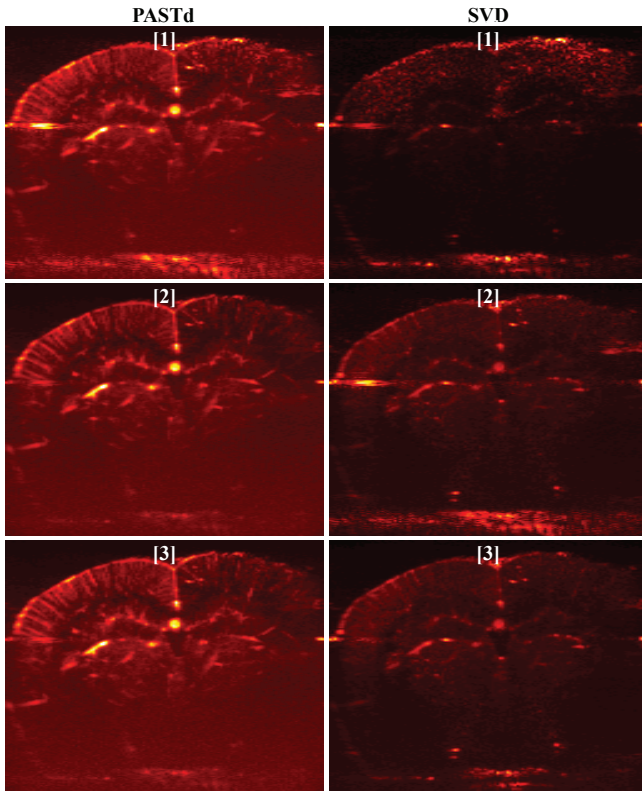


Figure 2: Comparing the exponentially weighted PASTd method and the SVD method by sequentially removing eigencomponents. The white number displays the number of removed components for each of the methods. It is clear that the exponential weighting of the PASTd method ($\beta = 0.5$) greatly reduces the number of components needed to remove.

B. Averaging

To reconstruct the blood flow signal, data from multiple time stamps is required. It is therefore conventional to average over a larger number of frames. In the batch-SVD method an average is taken over the same ensemble length where the SVD is calculated from. As the PASTd algorithm processes images sequentially and outputs frames at the same rate, any number of these can be stacked for averaging. While it is true that the output of the SVD can also be stacked, after which a different averaging filter length can be used, the effects caused by the non-continuity of the processing method need to be further investigated. These effects do not occur using the PASTd method as for example using PASTd-sw, every output frame is reconstructed using information from the last l frames. Implementing an SVD with a sliding window (SVD-sw), where a new image is created for every new input frame, is also not practical due to the high computational complexity and real-time constraints of Doppler imaging.

Averaging has a massive impact on the SNR of the PDI. When used in fUS, the temporal changes of a PDI pixel are correlated with a known stimulus pattern. A smoothing filter, such as a moving average, greatly increases the output Pearson correlation coefficient as shown in the Results section.

C. Adaptive thresholding

As the PASTd algorithm estimates eigencomponents, it is possible to adaptively threshold between different subspaces in a similar fashion to the SVD method. Even in the case of a reasonably stationary environment, the number of tissue components are not known *a priori* so it can be deduced using the eigenvalue magnitudes. It has also been shown that there can be a need for adaptive thresholding when strong tissue movement occurs during a measurement [5].

The PASTd method only calculates an estimate of the first r eigencomponents and, therefore, adaptive thresholding can only be done within these r components. In that sense, r has to be set sufficiently large for adaptive thresholding. Various methods to adaptively threshold for Doppler imaging have been proposed by Baranger *et al.* [5].

IV. RESULTS

To showcase the capabilities of the subspace tracking methods, the PASTd algorithm (with both a sliding window and exponential window) were implemented on a fUS dataset.

A. Convergence

For the application of fUS it is important to display accurate PDIs as soon as possible in real time. As the threshold between the tissue and blood subspaces is not always clearly defined and may vary from frame to frame, finding an objective performance measure is not trivial. We chose to calculate the MSE between the PDI created by the SVD-sw method and the PDIs from the PASTd-ew, PASTd-sw methods. Here, the SVD-sw method ($r = 15$, $n_e = 150$) is taken as ground truth. While this is of course not ideal it does give an indication of the convergence of the implemented methods to PDIs containing blood flow information.

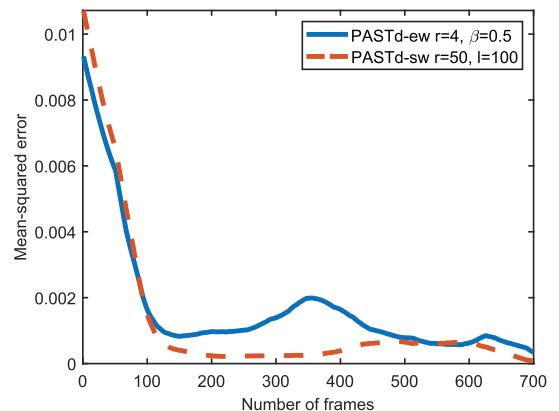


Figure 3: Comparing the convergence of the sliding window and exponential window PASTd PDIs compared to the state-of-the-art SVD method PDIs. Both methods remove the tissue subspace in a suitable time to be used for ultrafast Doppler imaging.

The displayed convergence plots were chosen based on a subjective evaluation of the reconstructed PDIs as they both accurately removed the tissue subspace. The settings were chosen as follows, PASTd-sw: $r = 30$, $l = 100$, PASTd-ew:

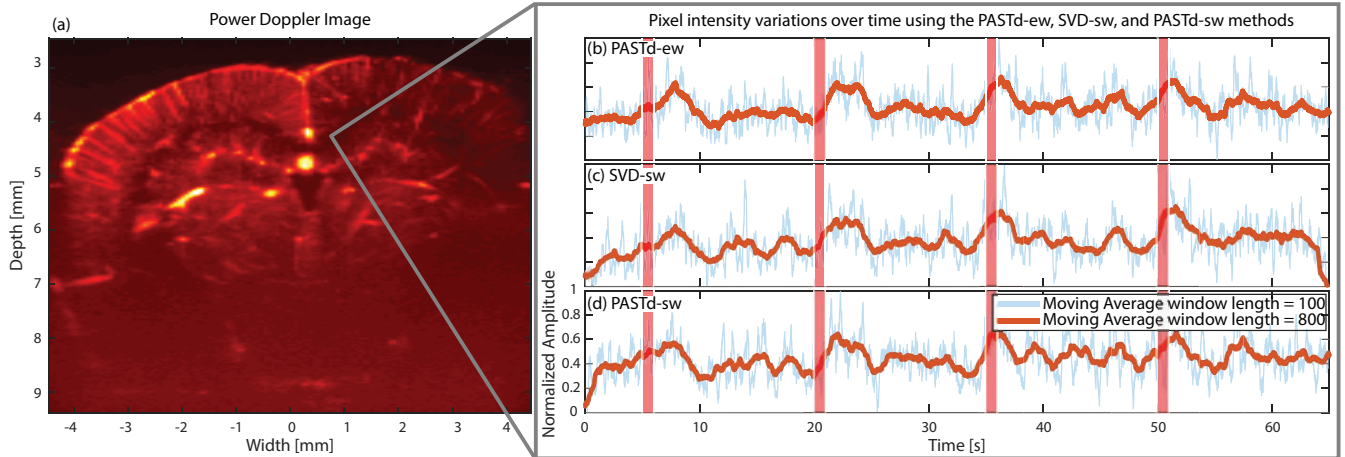


Figure 4: Efficient and flexible spatiotemporal clutter filtering of high frame rate images using subspace tracking. (a) shows a PDI of the vasculature of a mouse brain obtained with the PASTd method. (b)-(d) display the PDI pixel intensities over time during a fUS measurement using the exponentially weighted PASTd ($r = 5, \beta = 0.8$), sliding window SVD-sw ($r = 30, n_e = 150$), and sliding window PASTd ($r = 40, l = 60$) methods respectively. For each, moving average filters of length 100 and 800 are shown in light blue and orange respectively. The applied stimulation duration is shown in red.

$r = 3, \beta = 0.5$, both averaged over 150 frames. The results in Fig. 3 show that overall the PASTd-sw method converges to a lower MSE compared to the PASTd-ew window. This is not surprising as the SVD method is also implemented in a sliding window fashion though it does not necessarily mean the tissue subspace was more accurately removed. What can be noted is that for each method, a representation of the blood subspace is formed within a typical ensemble length of $n_e = 150$ frames and therefore the convergence is satisfactory for ultrafast Doppler imaging.

B. Functional Ultrasound

For fUS, the temporal information of every pixel is correlated with a known stimulus pattern [7]. The results of this experiment are shown in Fig. 4. An example PDI is shown in Fig. 4 (a) while Fig. 4 (b) - (d) show for the different methods, the intensity variations over time for one PDI pixel during a functional measurement. The Pearson correlation coefficients of the PASTd-ew, PASTd-sw, and SVD-sw method are 0.636, 0.525, and 0.569 respectively when using a moving average filter of length 800 for each method. These results highlight the potential of the PASTd method for use in ultrafast Doppler imaging.

V. CONCLUSION & DISCUSSION

PAST methods show potential for application in the field of ultrafast Doppler imaging. The created PDIs are of a similar quality to the current state-of-the-art SVD method while maintaining a lower computational complexity of $O(nr)$ per image for the PASTd-ew method versus $O(n \times n_e^2)$ per ensemble of images for the SVD method. Due to the exponential weighting of the PASTd method, only a few eigencomponents need to be removed to discard the clutter signals associated with slow moving tissue, which also contributes to a low computational complexity.

For a more accurate performance measure, convergence tests should be performed on a simulated dataset where the inputs are known. With a simulated dataset, the properties of each of the methods can be accurately tested and the current subjectivity of the results can be removed. This is reserved for future work.

While the advantages of processing the frames sequentially has to be further investigated using datasets with known inputs, the initial results on a fUS dataset look promising as larger Pearson correlation coefficients have been obtained compared to the current state-of-the-art SVD method.

REFERENCES

- [1] J. Bercoff, G. Montaldo, T. Loupas, D. Savery, F. Mzire, M. Fink, and M. Tanter, "Ultrafast compound Doppler imaging: Providing full blood flow characterization," *IEEE transactions on ultrasonics, ferroelectrics, and frequency control*, vol. 58, no. 1, 2011.
- [2] G. Montaldo, M. Tanter, J. Bercoff, N. Benech, and M. Fink, "Coherent plane-wave compounding for very high frame rate ultrasonography and transient elastography," *IEEE Trans Ultrason Ferroelectr Freq Control*, vol. 56, no. 3, pp. 489–506, Mar. 2009.
- [3] Y. M. Yoo, R. Managuli, and Y. Kim, "Adaptive clutter filtering for ultrasound color flow imaging," *Ultrasound in Medicine and Biology*, vol. 29, no. 9, pp. 1311–1320, Sep. 2003. [Online]. Available: [https://www.umbjournal.org/article/S0301-5629\(03\)01014-7/abstract](https://www.umbjournal.org/article/S0301-5629(03)01014-7/abstract)
- [4] C. Demen, T. Deffieux, M. Pernot, B. F. Osmanski, V. Biran, J. L. Gennisson, L. A. Sieu, A. Bergel, S. Franqui, J. M. Correias, I. Cohen, O. Baud, and M. Tanter, "Spatiotemporal Clutter Filtering of Ultrafast Ultrasound Data Highly Increases Doppler and fUltrasound Sensitivity," *IEEE Transactions on Medical Imaging*, vol. 34, no. 11, pp. 2271–2285, 2015.
- [5] J. Baranger, B. Arnal, F. Perren, O. Baud, M. Tanter, and C. Demen, "Adaptive spatiotemporal SVD clutter filtering for Ultrafast Doppler Imaging using similarity of spatial singular vectors," *IEEE Transactions on Medical Imaging*, vol. PP, no. 99, pp. 1–1, 2018.
- [6] Y. Bin, "Projection approximation subspace tracking," *IEEE Transactions on Signal Processing*, vol. 43, no. 1, pp. 95–107, 1995.
- [7] E. Macé, G. Montaldo, I. Cohen, M. Baulac, M. Fink, and M. Tanter, "Functional ultrasound imaging of the brain," *Nature Methods*, vol. 8, no. 8, pp. 662–664, Aug. 2011. [Online]. Available: <https://www.nature.com/articles/nmeth.1641>